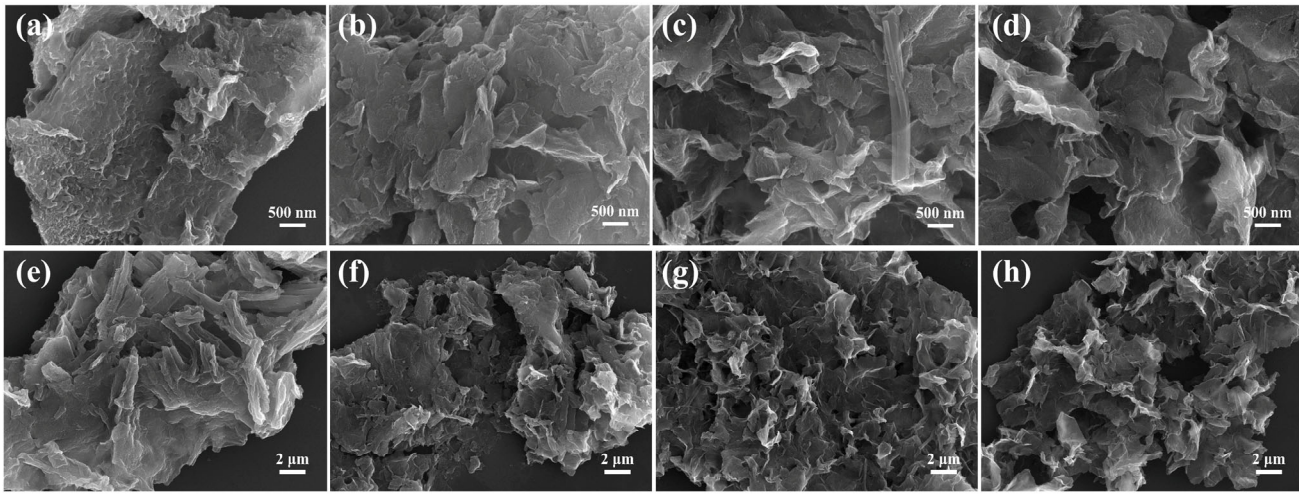

Figure S1. SEM images of (**a**,**e**) PDI-EDA, (**b**,**f**) PDI-EDA/EG-10, (**c**,**g**) PDI-EDA/EG-20, and (**d**,**h**) PDI-EDA/EG-30 composites, respectively.

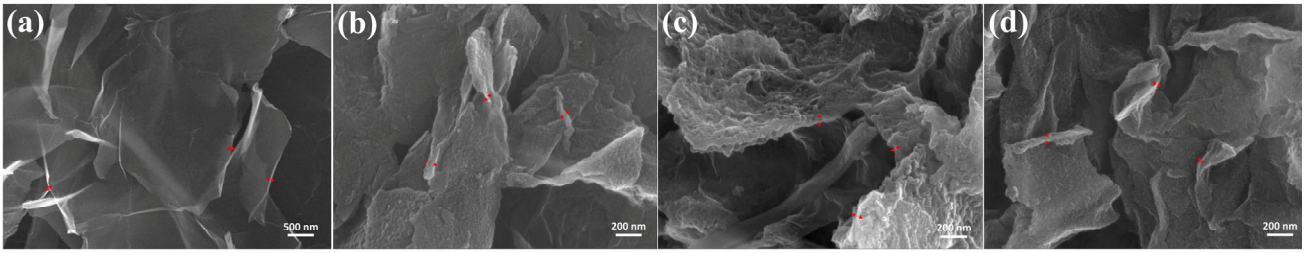

Figure S2. SEM images of (**a**) EG, (**b**) PDI-EDA/EG-10, (**c**) PDI-EDA/EG-20, and (**d**) PDI-EDA/EG-30 composites, respectively.

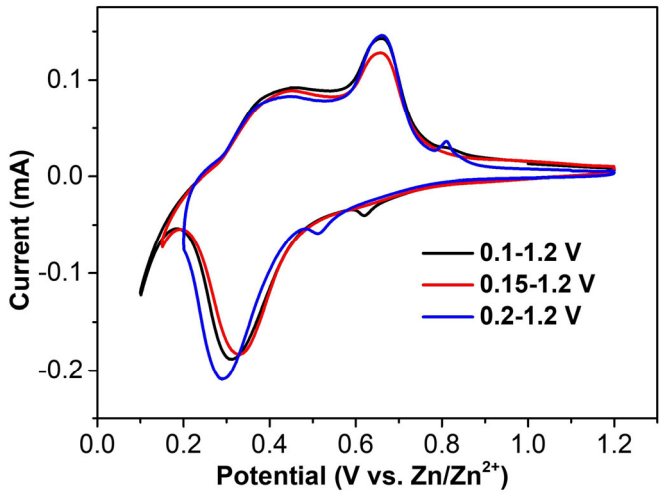

Figure S3. CV curves of the PDI-EDA/EG-20 electrode at different potential windows.

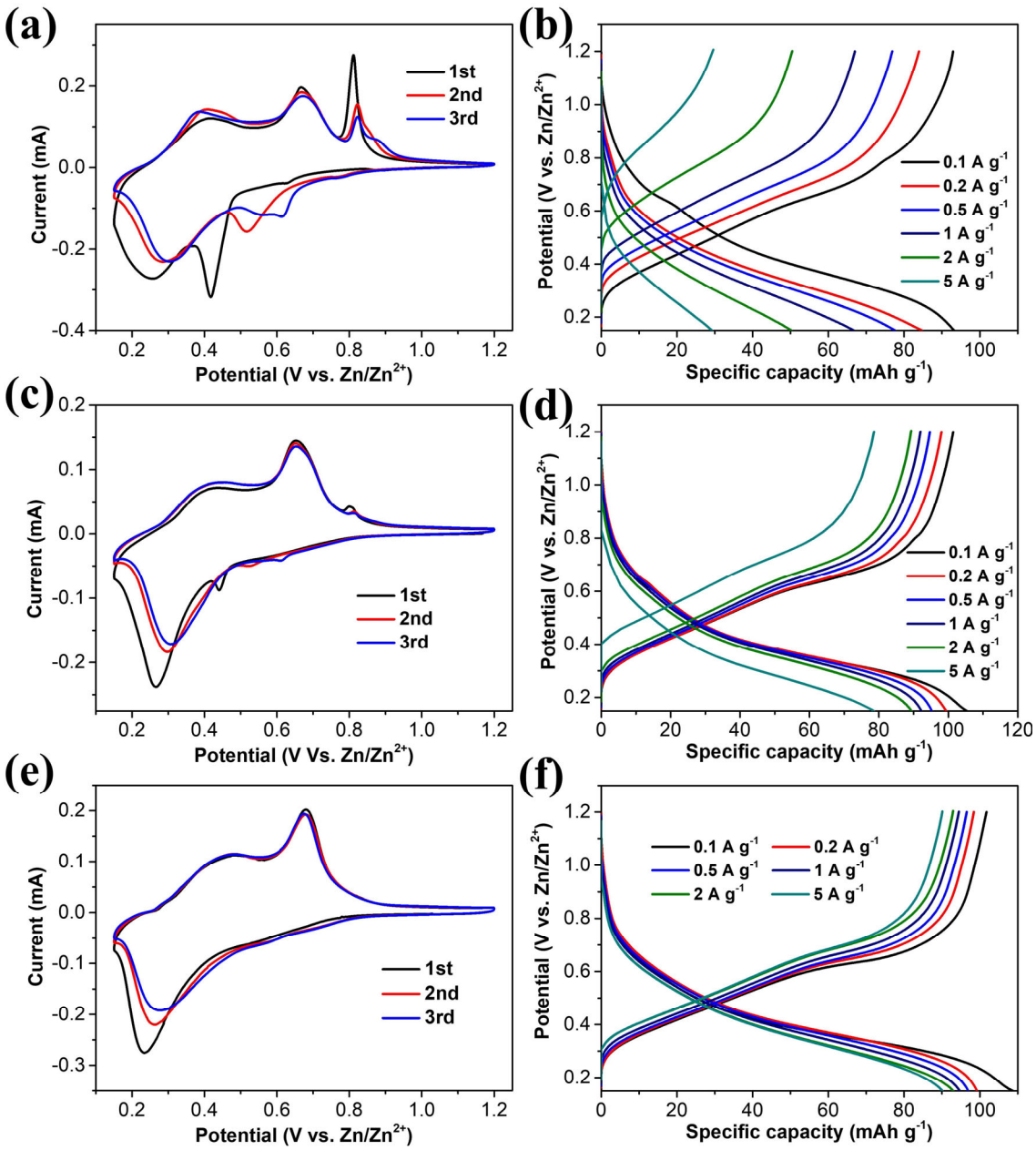

Figure S4. (**a**,**c**,**e**) CV curves and (**b**,**d**,**f**) GCD profiles of pure PDI-EDA, PDI-EDA/EG-10, and PDI-EDA/EG-20 electrodes, respectively.

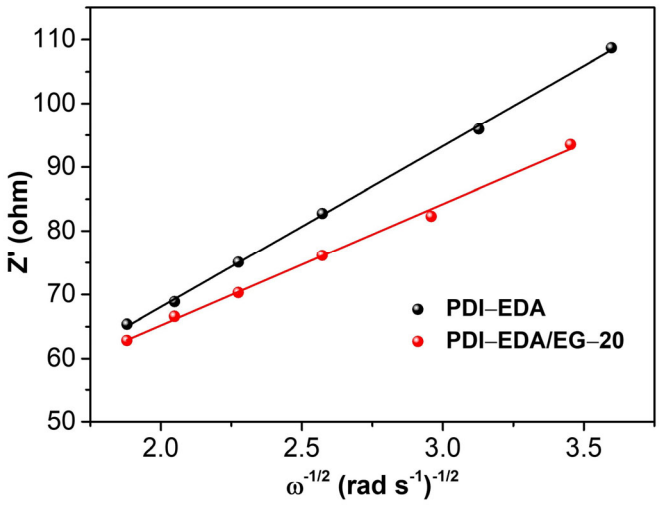

Figure S5. The relationship between Z′ and $w^{-1/2}$ for the PDI-EDA and PDI-EDA/EG-20 electrodes.

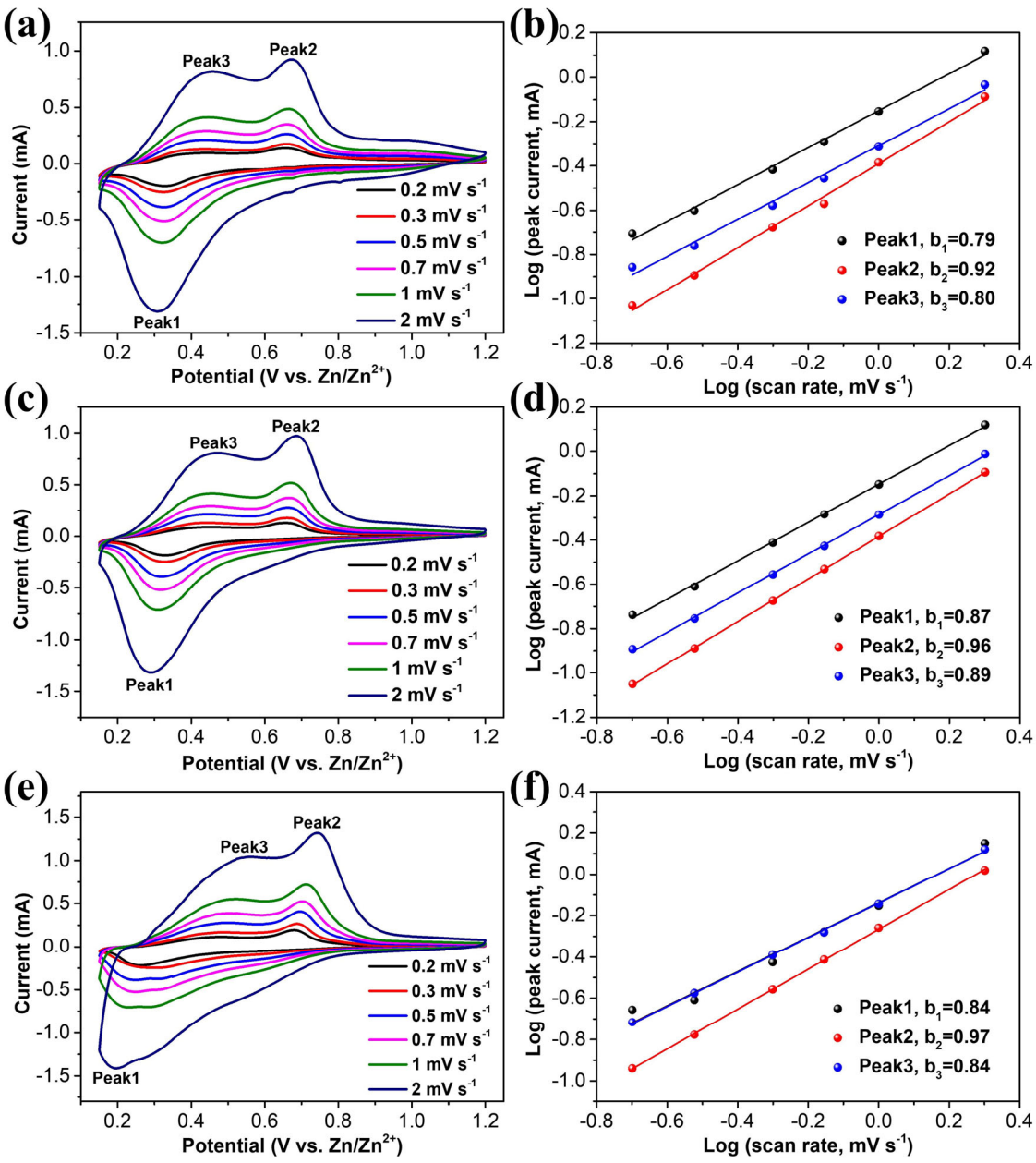

Figure S6. (**a**,**c**,**e**) CV curves at different current densities and (**b**,**d**,**f**) b values for anodic and cathodic peaks of PDI-EDA, PDI-EDA/EG-10, and PDI-EDA/EG-20 electrodes, respectively.

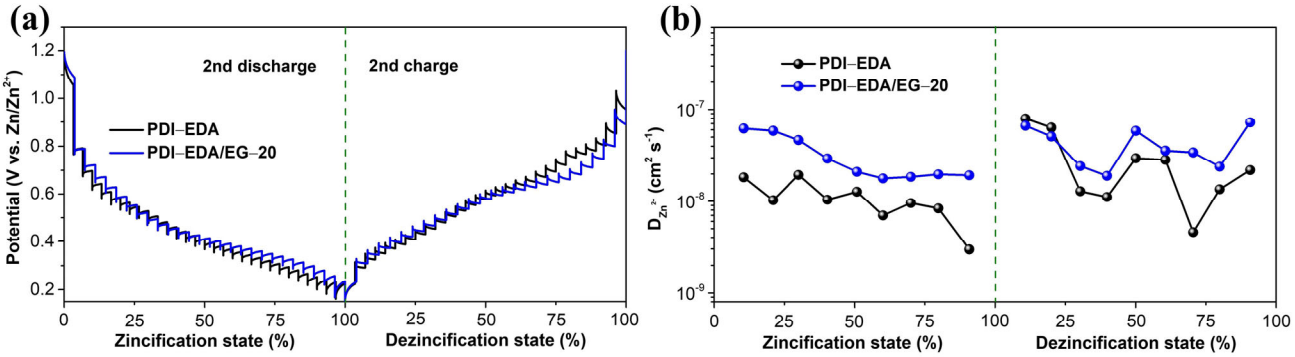

Figure S7. (**a**) GITT curves and (**b**) corresponding Zn^{2+} diffusion coefficients at different potential states.

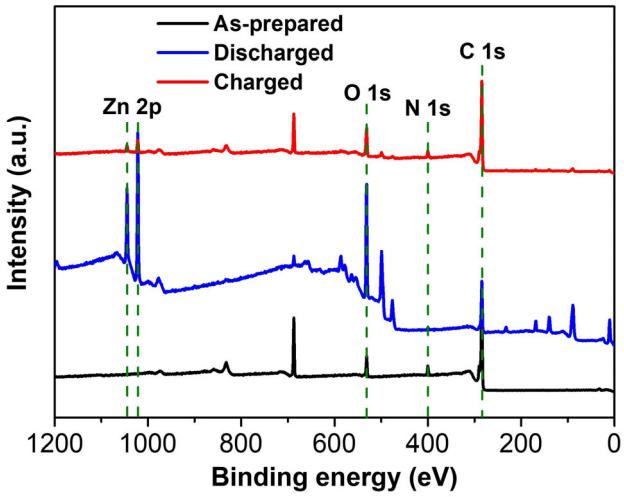

Figure S8. Typical XPS survey of the PDI-EDA/EG-20 electrode at different discharge/charge states.

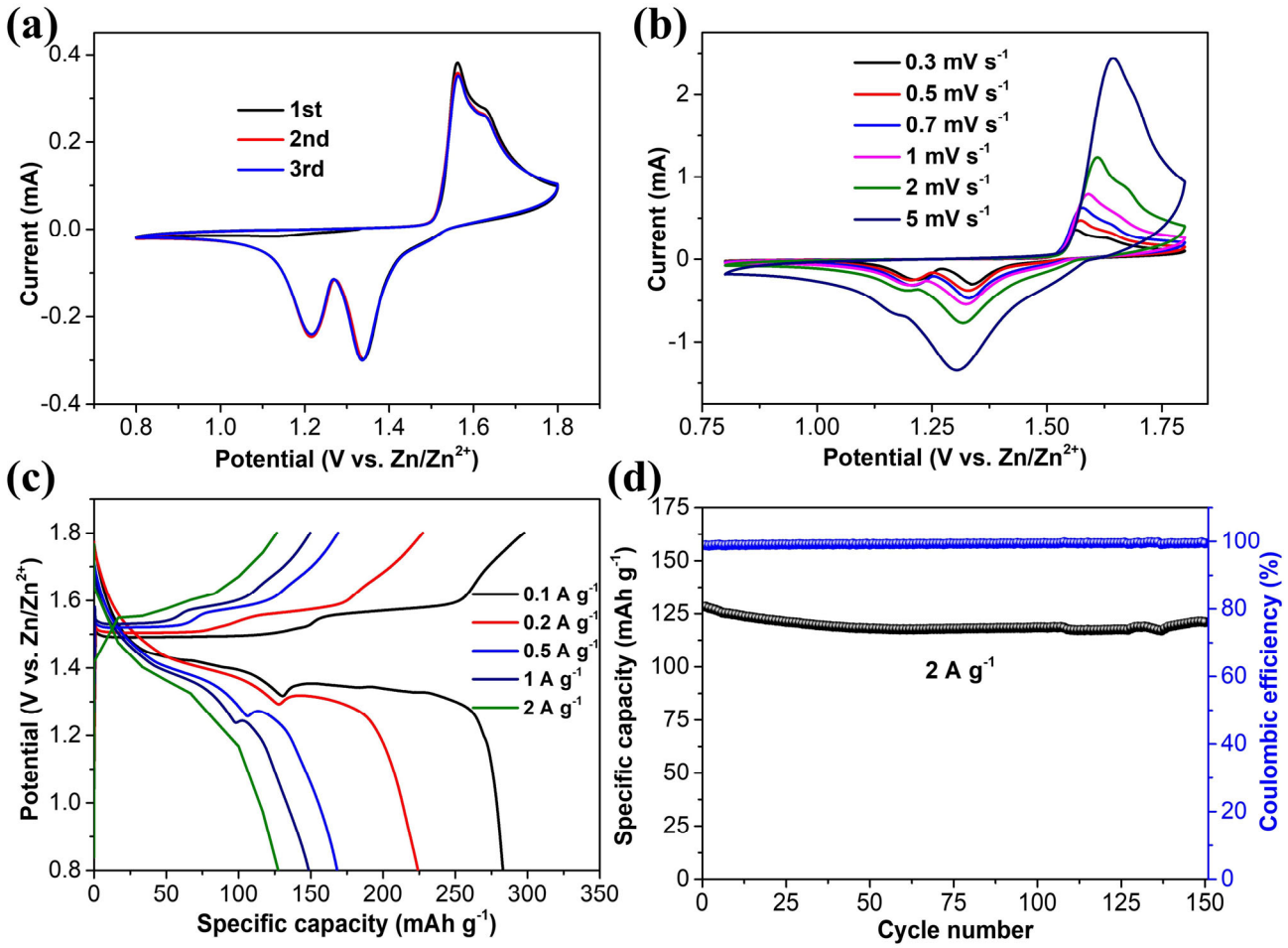

Figure S9. Electrochemical performance of the MnO_2 cathode. (**a**) Initial three CV curves. (**b**) CV curves at different sweep rates. (**c**) GCD profiles at different current densities. (**d**) Long-term cycling stability at 2 A g^{-1}.

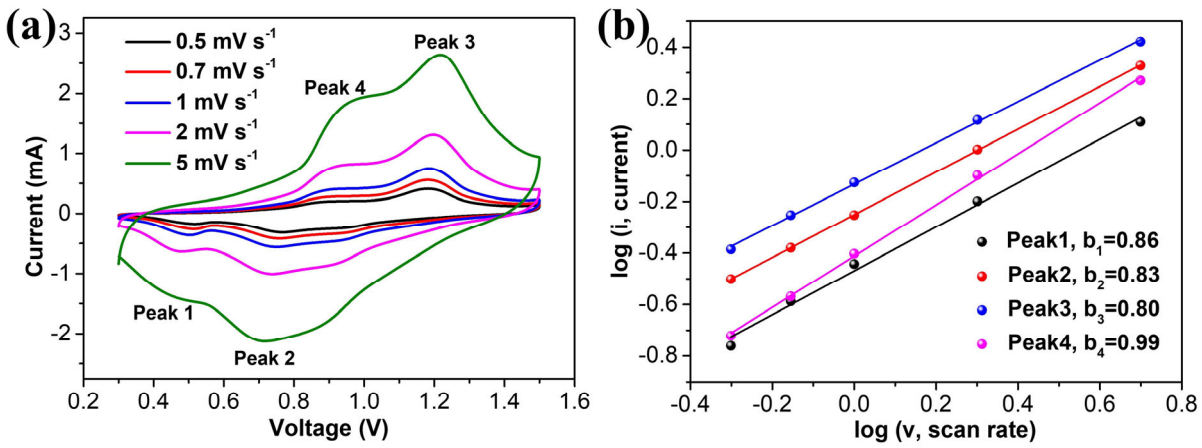

Figure S10. (**a**) CV curves of the device at different scan rates. (**b**) b values for cathodic and anodic peaks of the ZIB cell.

Table S1. Comparison of cycling performance of recently reported organic materials for ZIBs in the literature.

Organic Material.	Electrolyte	Cycle number	Capacity Retention	Ref.
PDI-EDA/EG	2 M $ZnSO_4$	1000, 1 A g^{-1}	93.4%	This work
PTVE	1 M $ZnSO_4$	500, 1 A g^{-1}	65%	[1]
BDB	19 M LiTFSI+1 M $Zn(OTF)_2$	1000, 0.78 A g^{-1}	75%	[2]
PANI	1 M $Zn(OTF)_2$	3000, 5 A g^{-1}	92%	[3]
PT	1 M $Zn(OTF)_2$	550, 0.1 A g^{-1}	61.86%	[4]
C4Q	3 M $Zn(OTF)_2$	1000, 0.5 A g^{-1}	87%	[5]
PTO	2 M $ZnSO_4$	1000, 3 A g^{-1}	70%	[6]
CMP	2 M $ZnCl_2$	1000, 6 A g^{-1}	87.6%	[7]
poly(1,5-NAPD)/Poly(pAP)	2 M $ZnSO_4$	5000, 5 A g^{-1}	88%	[8]
PTA-026	3 M $ZnSO_4$	200, 0.8 A g^{-1}	92.2%	[9]
BQPH	2 M $ZnSO_4$	1000, 10 A g^{-1}	82%	[10]

References

1. Luo, Y.; Zheng, F.; Liu, L.; Lei, K.; Hou, X.; Xu, G.; Meng, H.; Shi, J.; Li, F. A High-Power Aqueous Zinc-Organic Radical Battery with Tunable Operating Voltage Triggered by Selected Anions. *ChemSusChem* **2020**, *13*, 2239–2244.
2. Glatz, H.; Lizundia, E.; Pacifico, F.; Kundu, D. An Organic Cathode Based Dual-Ion Aqueous Zinc Battery Enabled by a Cellulose Membrane. *ACS Appl. Energ. Mater.* **2019**, *2*, 1288–1294.
3. Wan, F.; Zhang, L.; Wang, X.; Bi, S.; Niu, Z.; Chen, J. An Aqueous Rechargeable Zinc-Organic Battery with Hybrid Mechanism. *Adv. Funct. Mater.* **2018**, *28*, 1804975.
4. Wu, M.; Su, W.; Wang, X.; Liu, Z.; Zhang, F.; Luo, Z.; Yang, A.; Yeleken, P.; Miao, Z.; Huang, Y. Long-Life Aqueous Zinc-Organic Batteries with a Trimethyl Phosphate Electrolyte and Organic Cathode. *ACS Sustain. Chem. Eng.* **2023**, *11*, 957–964.
5. Zhao, Q.; Huang, W.; Luo, Z.; Liu, L.; Lu, Y.; Li, Y.; Li, L.; Hu, J.; Ma, H.; Chen, J. High-capacity aqueous zinc batteries using sustainable quinone electrodes. *Sci. Adv.* **2018**, *4*, eaao1761.
6. Guo, Z.; Ma, Y.; Dong, X.; Huang, J.; Wang, Y.; Xia, Y. An Environmentally Friendly and Flexible Aqueous Zinc Battery Using an Organic Cathode. *Angew. Chem. Int. Ed.* **2018**, *130*, 11911–11915.
7. Zhang, H.; Zhong, L.; Xie, J.; Yang, F.; Liu, X.; Lu, X. A COF-Like N-Rich Conjugated Microporous Polytriphenylamine Cathode with Pseudocapacitive Anion Storage Behavior for High-Energy Aqueous Zinc Dual-Ion Batteries. *Adv. Mater.* **2021**, *33*, 2101857.
8. Zhao, Y.; Huang, Y.; Wu, F.; Chen, R.; Li, L. High-Performance Aqueous Zinc Batteries Based on Organic/Organic Cathodes Integrating Multiredox Centers. *Adv. Mater.* **2021**, *33*, 2106469.
9. Wang, X.; Wang, G.; He, X. Anthraquinone porous polymers with different linking patterns for high performance Zinc-Organic battery. *J. Colloid Interf. Sci.* **2023**, *629*, 434–444.
10. Tie, Z.; Zhang, Y.; Zhu, J.; Bi, S.; Niu, Z. An Air-Rechargeable Zn/Organic Battery with Proton Storage. *J. Am. Chem. Soc.* **2022**, *144*, 10301–10308.